Constitutive centromere-associated network controls centromere drift in vertebrate cells

Tetsuya Hori,[1] Naoko Kagawa,[2] Atsushi Toyoda,[3] Asao Fujiyama,[3,4] Sadahiko Misu,[5] Norikazu Monma,[5] Fumiaki Makino,[1] Kazuho Ikeo,[5] and Tatsuo Fukagawa[1]

[1]Graduate School of Frontier Biosciences, Osaka University, Suita, Osaka 565-0871, Japan
[2]Department of Molecular Genetics, National Institute of Genetics and The Graduate University for Advanced Studies (SOKENDAI), Mishima, Shizuoka 411-8540, Japan
[3]Comparative Genomics Laboratory, National Institute of Genetics, Mishima, Shizuoka 411-8540, Japan
[4]National Institute of Informatics, Chiyoda-ku, Tokyo 101-8430, Japan
[5]DNA Data Analysis Laboratory, National Institute of Genetics, Mishima, Shizuoka 411-8540, Japan

Centromeres are specified by sequence-independent epigenetic mechanisms, and the centromere position may drift at each cell cycle, but once this position is specified, it may not be frequently moved. Currently, it is unclear whether the centromere position is stable. To address this question, we systematically analyzed the position of nonrepetitive centromeres in 21 independent clones isolated from a laboratory stock of chicken DT40 cells using chromatin immunoprecipitation combined with massive parallel sequencing analysis with anti–CENP-A antibody. We demonstrated that the centromere position varies among the clones, suggesting that centromere drift occurs during cell proliferation. However, when we analyzed this position in the subclones obtained from one isolated clone, the position was found to be relatively stable. Interestingly, the centromere drift was shown to occur frequently in CENP-U– and CENP-S–deficient cells. Based on these results, we suggest that the centromere position can change after many cell divisions, but this drift is suppressed in short-term cultures, and the complete centromere structure contributes to the suppression of the centromere drift.

Introduction

The centromere is a critical genomic region where the kinetochore is assembled and mediates the interaction between chromosome and spindle microtubules in the process of faithful chromosome segregation. The centromere position must be specified at a single locus on each chromosome to prevent chromosome instability in most organisms, and the specification of the centromere position is an important step during chromosome segregation. Centromeres with repetitive sequences are found in many organisms (Fukagawa and Earnshaw, 2014a). For example, most human and mouse chromosomes contain α satellite and minor satellite sequences, respectively. Although DNA sequence may contain information significant for the centromere function, a recent consensus theory suggests that the DNA sequence itself is not crucial for the centromere specification, but that the centromere is specified at a particular position by sequence-independent epigenetic mechanisms (Allshire and Karpen, 2008; Perpelescu and Fukagawa, 2011; Fukagawa and Earnshaw, 2014a). This theory is based on the discovery and characterization of human neocentromeres, which do not possess α satellite sequences, but contain most of the kinetochore components and can contribute to faithful chromosome segregation (Marshall et al., 2008; Fukagawa and Earnshaw, 2014b). A centromere-specific histone H3 variant, CENP-A, was identified at most centromeres described to date, including neocentromeres. Additionally, because CENP-A represents an upstream factor required for kinetochore assembly (McKinley and Cheeseman, 2016), it has recently been suggested that CENP-A carries an epigenetic mark for the centromere specification (Black and Cleveland, 2011; Westhorpe and Straight, 2013).

The formation of human neocentromeres is observed in some diseases (Voullaire et al., 1993; du Sart et al., 1997; Marshall et al., 2008; Fukagawa and Earnshaw, 2014b), and it is possible that the functional and structural aspects of neocentromeres are somewhat different from the naturally occurring centromeres. However, chromatin immunoprecipitation (ChIP) combined with massive parallel sequencing (ChIP-seq), using anti–CENP-A antibodies revealed the existence of native nonrepetitive centromeres at horse (Wade et al., 2009), chicken (Shang et al., 2010, 2013), and orangutan (Lomiento et al., 2013) chromosomes. Because these nonrepetitive centromeres are functional, this suggests that they are functionally equivalent to the centromeres with repetitive sequences.

In general, the characterization of centromeric chromatin is difficult because of the existence of highly repetitive sequences. The mapping of DNAs obtained by ChIP experiments

Correspondence to Tatsuo Fukagawa: tfukagawa@fbs.osaka-u.ac.jp

Abbreviations used: CCAN, constitutive centromere-associated network; ChIP, chromatin immunoprecipitation.

The Rockefeller University Press $30.00
J. Cell Biol. Vol. 216 No. 1 101–113
https://doi.org/10.1083/jcb.201605001

with anti-centromere antibodies to the repetitive regions is difficult to perform. Therefore, the use of nonrepetitive centromeres allows the precise mapping of DNA molecules precipitated using ChIP to nonrepetitive centromeres, which makes native nonrepetitive centromeres a very useful model for the characterization of centromeric chromatin. For example, using this nonrepetitive feature, CENP-A distribution in centromeric chromatin can be investigated at the base pair resolution.

Previous ChIP-on-chip analyses, using anti–horse CENP-A antibody, indicated that CENP-A is located at the 100–160-kb nonrepetitive region of horse chromosome 11 (Wade et al., 2009; Purgato et al., 2015). Analysis of five different horse cell lines indicated that the CENP-A–associated region varies among these lines (Purgato et al., 2015), suggesting a potential drift of centromere position. The centromere drift was suggested to occur at the fission yeast central core sequence as well (Yao et al., 2013). In contrast to this, centromere position was shown to be relatively stable in maize inbred lines with one common parent (Gent et al., 2015). This centromere drift is possible because centromeres are specified by sequence-independent mechanisms. However, it may also be possible that this position, once specified, does not drift frequently, because neocentromeres are generated rarely. Understanding the control of centromere specification and stability remains an unresolved issue, and a systematic approach should be used to address this question.

In this study, we isolated 21 independent clones from a laboratory stock of wild-type chicken DT40 cells and examined the position of nonrepetitive centromere Z in each clone using ChIP-seq analysis with anti–CENP-A antibodies. We found that this position varies between the clones, indicating a centromere drift. However, centromere positions in the subclones obtained from one of the isolated clones were shown to be stable. Interestingly, the centromere drift was shown to occur frequently in CENP-U– and CENP-S–deficient cells (Minoshima et al., 2005; Hori et al., 2008b; Amano et al., 2009), which are viable, but have partially disrupted centromere structure. Collectively, these results indicate that the centromere drift can occur during cell proliferation, but the mechanisms of centromere drift suppression exist as well, and the complete centromere structure is critical for the regulation of the centromere position.

Results

Centromere drift occurs during cell proliferation of wild-type DT40 cells

Nonrepetitive centromeres were found at chicken chromosomes Z, 5, and 27 (Shang et al., 2010), and therefore we characterized the position and size of these nonrepetitive centromeres at base pair resolution using ChIP-seq analysis with anti–CENP-A antibody. Because the size and position of centromeres may vary depending on the chosen method of examination, we defined a method, presented in Fig. S1 (A and B), and used it consistently throughout the study. As DT40 cells have two copies of chromosomes 5 and 27, it is possible that the centromere position of each allele may not be identical, as observed in the horse chromosome 11 (Wade et al., 2009; Purgato et al., 2015), which complicates the analysis and evaluation of the obtained results. Therefore, we focused on chromosome Z, a single-copy chromosome in DT40 cells, which facilitates the observations of the centromere position at this chromosome.

When we compared the chromosome Z centromere size in the cells from two different laboratory stocks of the wild-type DT40 cells (lot 110114 and lot 140806), we showed that the size of centromere Z differed slightly between these lots (41.5 kb in lot 110114 cells and 49.1 kb in lot 140806 cells; Fig. 1 A). Lot 140806 cells originated from lot 110114 cells, and they cultured at least several months longer than the cells from the lot 110114 cells, which led to the increase in the centromere size. Culturing of these cells may lead to a change in chromosome Z copy numbers or cause chromosome rearrangements. We performed FISH analysis using a chromosome Z–specific probe. In ∼97% of cell populations, we detected a single chromosome Z (Fig. S2 A), indicating chromosome instability does not occur in culture of lot 140806 cells.

We have previously established an experimental system in which the centromere is conditionally removed, and neocentromeres are isolated at various positions on chromosome Z (Shang et al., 2013). Analyzing these neocentromeres with ChIP-seq using anti–CENP-A antibody, we found that the sizes of the CENP-A–associated regions in neocentromeres are remarkably similar (Shang et al., 2013), suggesting that centromere size is tightly regulated in chicken cells. However, in this study, we found that the size of CENP-A–associated regions increases during cell culture (Fig. 1 A), suggesting that centromere drift occurs over many cell divisions, and that the CENP-A–associated region size we observed represents a mixture of centromeres at different positions rather than the expansion of a single centromere (Fig. 1 B). The characterization of the chromosome Z centromere size in DT40 cells obtained from another laboratory (DT40 Oxford; provided by W. Brown, The University of Nottingham, Nottingham, England, UK) showed that the position of centromere Z in DT40 Oxford cells differs from the positions previously observed in our laboratory stocks (Fig. S1 C), which supports our hypothesis.

To further examine this hypothesis, we isolated 21 independent clones from parental wild-type DT40 cells (lot 140806), and ChIP-seq analysis demonstrated that the size of CENP-A–associated region increased in these cells (Fig. 1, A and C). Additionally, we confirmed that the centromere size and position did not change during only 2 wk of wild-type DT40 cell culture (see Centromere drift is limited immediately after cloning), and therefore, we investigated the possibility of centromere drift during cell culture before cloning (Fig. 1 C). As shown in Fig. 1, D and E, parental cell centromere size (49.1 kb) was shown to be greater than the mean size of centromeres of the newly isolated clones (33.4 kb). The centromere size of each clone (CENP-A peak width) is plotted in Fig. 1 E. Additionally, we demonstrated that the centromere position differs among the clones (Fig. 1, D and F), as we defined the centromere position as a center of CENP-A–associated region and found that this position in each clone drifted within a 16.8-kb region (Fig. 1 F). We isolated clones in which centromeres were drifted at the right side of centromere Z, whereas we did not find clones with a centromere drift at left side (Fig. 1 F). This may be related to the existence of heterochromatin at the left side of centromere Z. Consistent with this explanation, a heterochromatin marker, H3K27me3, was slightly enriched at the left side of centromere Z (Fig. 1 F). Although our analyses focused on the nonrepetitive centromere Z, we detected centromere drift in the repetitive centromere 1 as well (Fig. S2, B and C). Chicken chromosome 1 centromere contains repetitive sequences, which span 350–450 kb (Shang et al., 2010). The CENP-A–associated

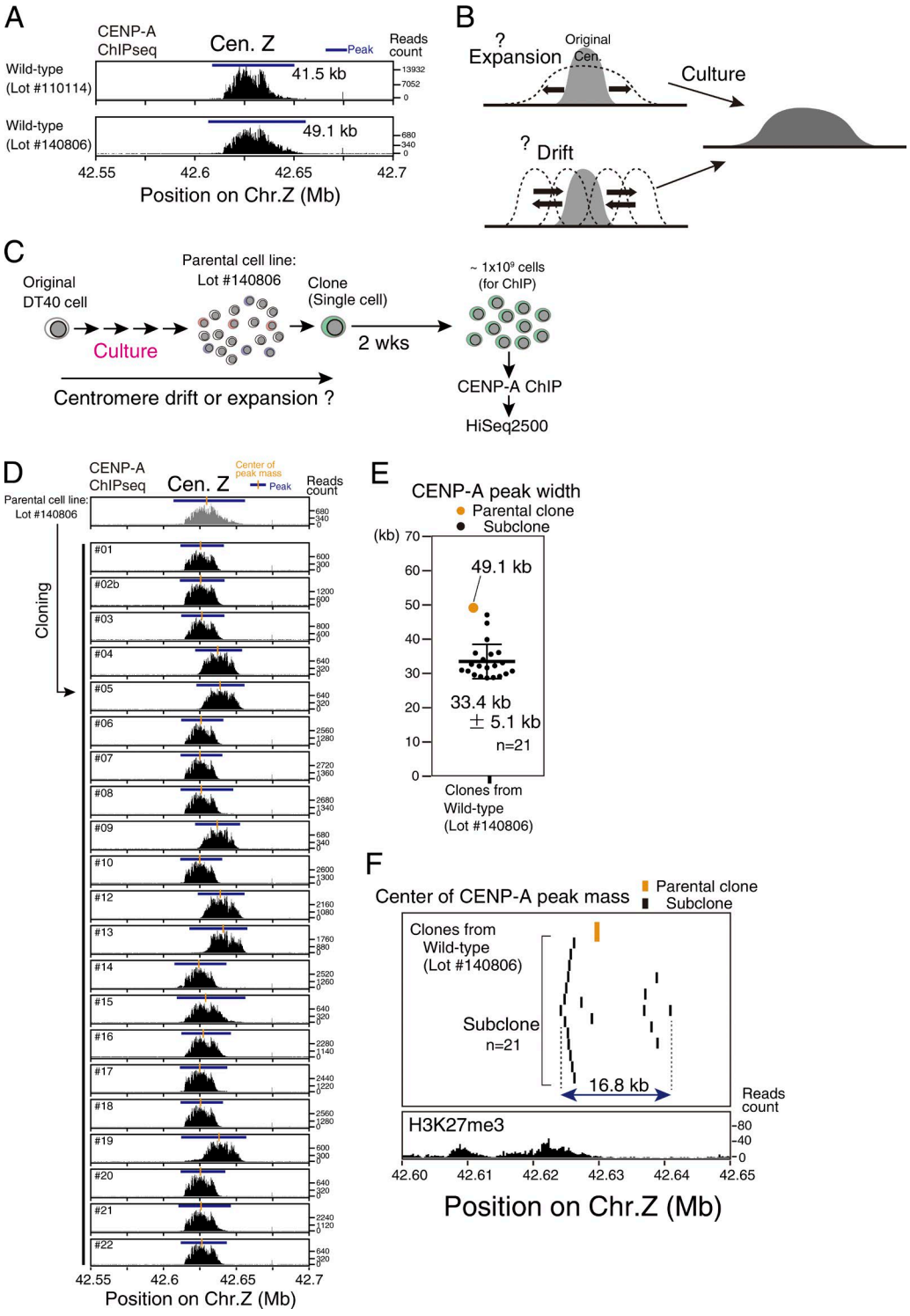

Figure 1. **Centromeres drift during cell proliferation of wild-type DT40 cells.** (A) ChIP-seq profiles of CENP-A at chicken chromosome Z in two independent DT40 batches. Two laboratory stocks of DT40 cells were maintained through different numbers of cell divisions. Centromere sizes in the lots 110114 and 140806 cells were 41.5 and 49.1 kb, respectively. Defined CENP-A peak ranges are indicated by blue bars. (B) Two possible explanations of the wider CENP-A distribution, based on ChIP-seq analysis. (C) Cloning strategy. After the primary cloning, 21 independent clones of the wild-type DT40 cells were isolated and subjected to ChIP-seq analysis using anti–CENP-A antibody. (D) ChIP-seq profiles of CENP-A at chicken chromosome Z in 21 independent clones isolated from a laboratory stock of DT40 cells (lot 140806). Defined CENP-A peak ranges and centers of peak mass are indicated by blue horizontal bars and orange vertical bars, respectively. (E) Centromere size (CENP-A peak width of centromere Z) in 21 clones, analyzed by ChIP-seq with anti–CENP-A antibody. Centromere size in the parental cells was 49.1 kb. Mean size and SD in 21 isolated clones was 33.4 ± 5.1 kb and is indicated by a thick horizontal bar and two thin horizontal bars, respectively. (F) The distribution of centromere position on chromosome Z in 21 isolated clones. The centromere position was defined as the center of peak mass obtained by CENP-A ChIP-seq analysis. Centromere position drifted in 16.8-kb region. ChIP-seq profiles of H3K27me3 in wild-type DT40 cells are also shown. H3K27me3 was slightly enriched at left side of CENP-A peaks in 21 isolated clones.

region is located near the edge of the repetitive region, but it may span to the nonrepetitive region in some clones, indicating that centromere drift on chromosome 1 occurs in these clones (Fig. S2, B and C).

Based on these results, we suggest that although the centromere size remains constant, the centromere position changes over a large number of cell divisions during cell proliferation of wild-type DT40.

Centromere drift is limited immediately after cloning

Next, we tried to determine the stability of centromere position and the frequency of the centromere drift. The parental DT40 cells were obtained from one of our laboratory stocks, and the exact number of divisions since the establishment of the original DT40 cell line was unknown (Fig. 1 C). To examine the frequency of centromere drift, we reisolated additional subclones, originating from one isolated clone (Fig. 1 D; clone 02b) and performed further ChIP-seq analyses, examining centromere drift during a 2-wk culture (Fig. 2 A). As shown in Fig. 2 B, the mean centromere size (31.4 kb) of each subclone isolated from clone 02b is very similar to the centromere size of clone 02b (30.7 kb). Each centromere size (CENP-A peak width) of 17 clones is plotted in Fig. 2 C. Additionally, the centromere drift was shown to be limited in the newly isolated clones: centromere centers in each clone drifted only within a 4.2-kb region (Fig. 2 D), a range much shorter than the one previously determined for analysis of a laboratory stock (16.8 kb; Fig. 1 F). Approximately 2 wk were needed to isolate each subclones from single parental clone 02b (Fig. 2 A). Because the doubling time of DT40 cells is 8–10 h, we compared the centromere size and position of clone 02b with those of its subclones after 40–50 cell divisions and showed that the centromere size and position in clone 02b are similar to those of subclones (Fig. 2, B–D). This suggests that the centromere size and position are relatively stable through a small number of cell divisions (at least 40–50 divisions).

Centromere drift more frequently occurs in CENP-U– or CENP-S–deficient cells than in the wild-type DT40 cells

We attempted to elucidate the molecular basis underlying the maintenance of the stability of centromere position and size. CENP-A incorporation into centromeric chromatin is mediated by specific chaperone HJURP (Dunleavy et al., 2009; Foltz et al., 2009). HJURP directly binds the predeposition CENP-A–H4 complex, and CENP-A levels were shown to be dramatically reduced in HJURP-deficient cells. However, the characterization of the centromere position in HJURP-deficient cells using anti–CENP-A antibody is difficult. In addition to HJURP, CENP-H–associated proteins, the members of constitutive centromere-associated network (CCAN) proteins, are involved in the deposition of newly synthesized CENP-A into centromeres as well (Okada et al., 2006, 2009). Although many CCAN proteins and HJURP are essential for cell viability, CENP-O and CENP-S/X complex knockouts are viable (Minoshima et al., 2005; Hori et al., 2008b; Amano et al., 2009). However, as it is possible that CCAN organization is partially disturbed in these knockout cells, we investigated centromere drift in CENP-U– (a CENP-O complex member) or CENP-S–deficient cells.

Unlike the wild-type DT40 cells, CENP-U– and CENP-S–deficient cells used in the experiments originated from a relatively fresh cell stocks. However, even in this study, the centromeres of CENP-U– and CENP-S–deficient cells were shown to be longer than those of wild-type DT40 cells (67.2 and 58.6 kb, respectively), suggesting that the centromere drift may occur more frequently in CENP-U– and CENP-S–deficient cells (Fig. 3 A). Afterward, we isolated independent clones of both CENP-U– and CENP-S–deficient cells and examined the centromere size and position in each clone (Fig. 3 B). Similar to the results obtained previously (Figs. 1 and 2), the mean centromere size observed in these clones (44.9 kb in CENP-U knockout cells and 48.0 kb in CENP-S knockout cells) was lower than that measured in both CENP-U– and CENP-S–deficient parental cells (67.2 kb in CENP-U–deficient and 58.6 kb in CENP-S–deficient cells), and the centromere position was shown to vary among these clones (Fig. 3, C–E). However, the centromere size range in both CENP-U– (44.9 kb) and CENP-S–deficient (48.0 kb) clones was demonstrated to be greater than the mean size of new wild-type clones (33.4 kb; Figs. 1 E and 3 E). Additionally, the drift ranges in both CENP-U– and CENP-S–deficient cells were wider (33.0 kb in CENP-U–deficient cells and 22.1 kb in CENP-S–deficient cells) compared with the wild-type cells (16.8 kb; Fig. 1 F and Fig. 3, C, D, and F).

In addition to centromere drift in chromosome Z, we observed clear centromere drift in chromosome 5 in CENP-U–deficient cells (Fig. 4). As DT40 has two copies of chromosome 5, it is sometimes difficult to evaluate centromere drift in chromosome 5. However, we observed clear two centromere peaks or a broader peak that may be mixture of two alleles of the centromere peaks in chromosome 5 among independent clones from CENP-U–deficient cells (Fig. 4). It is hard to observe such kinds of peak profile in wild-type cells.

These results show that the centromeres drift more frequently in CENP-U– and CENP-S–deficient cells than in the wild-type DT40 cells.

Centromere drift occurs in CENP-U– or CENP-S–deficient cell cultures for 16 d

To elucidate how many cell divisions are necessary to lead to the centromere drift, we used CENP-U conditional knockout cells, in which CENP-U expression can be suppressed by the addition of tetracycline (Hori et al., 2008b), and performed ChIP-seq analyses with anti–CENP-A antibody at different time points after tetracycline addition (Fig. 5 A). Afterward, we compared the centromere size in these cells before and after tetracycline addition. Before tetracycline addition, the expression level of CENP-U in CENP-U conditional knockout cells was shown to be similar to that in wild-type cells, with the centromere size of 34.8 kb. This size did not change significantly after 16-d culture in the absence of tetracycline (16 d on). In contrast to this, the centromere size increased to 54.3 kb after 16-d culture in the presence of tetracycline (16 d off) and further to 59.3 kb after the additional 16 d in the presence of tetracycline (32 d off; Fig. 5, B and C). Furthermore, we analyzed the cells after 16-d culture in the presence of tetracycline and an additional 16 d in the absence of tetracycline (16 d off and 16 d on) to investigate the potential reversibility of centromere size (Fig. 5 A), and we demonstrated that the centromere size does not decrease in comparison with that in the cells cultured for 16 d in the presence of tetracycline (16 d off; Fig. 5, B and C). Therefore, we suggest that the observed increase of the centromere size in CENP-U–deficient cells is the result of the analysis of mixed cell populations, with the centromeres at different positions,

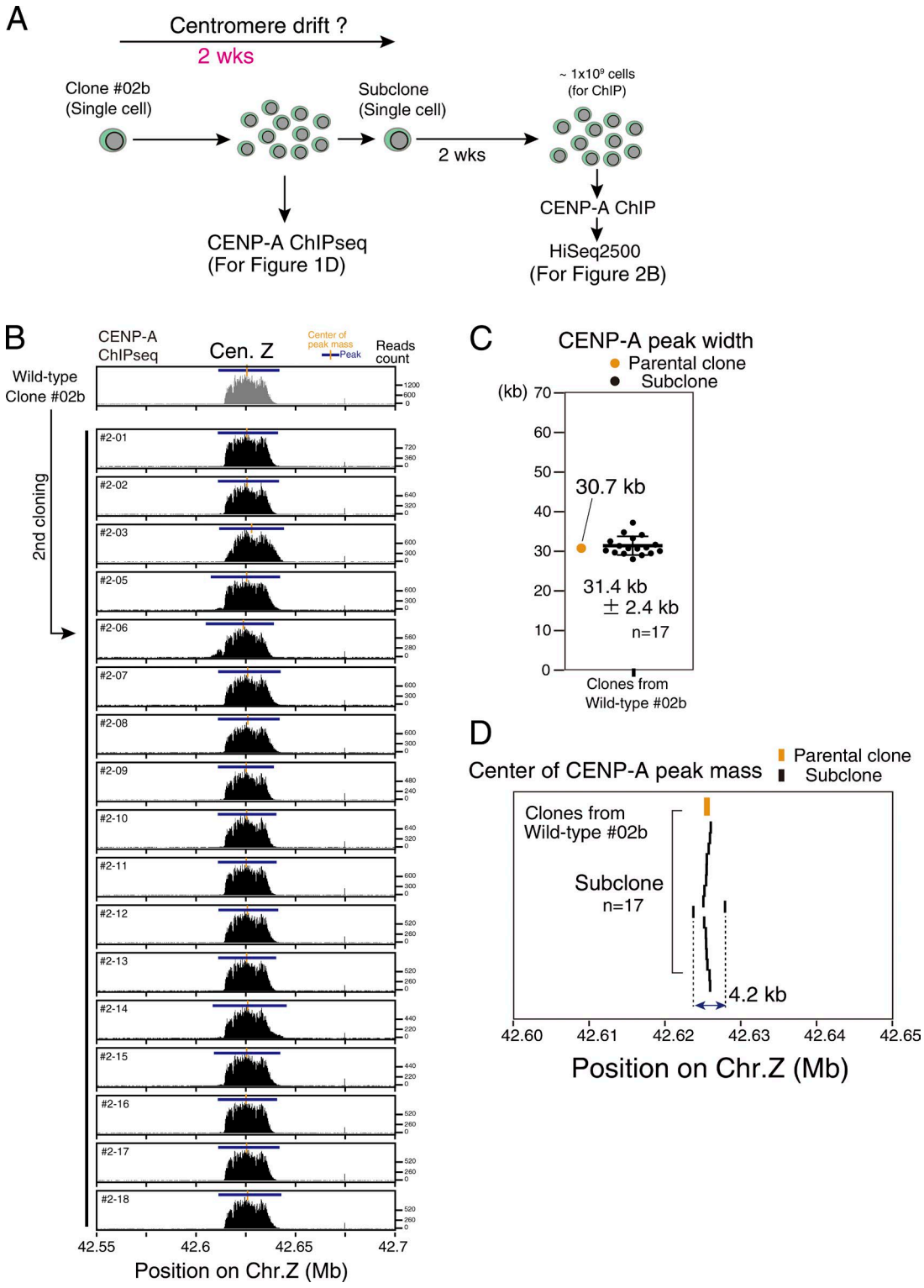

Figure 2. **Centromere-drift is limited immediately after the cloning of cells.** (A) Recloning strategy, using a previously isolated clone. Clone 02b was selected, and independent subclones were isolated for further ChIP-seq analyses using anti–CENP-A antibody. (B) ChIP-seq profiles of CENP-A on chicken chromosome Z in 17 independent subclones, isolated from clone 02b. Defined CENP-A peak ranges and centers of peak mass are indicated by blue horizontal bars and orange vertical bars, respectively. (C) Centromere size (CENP-A peak width of centromere Z) in 17 subclones, analyzed using ChIP-seq with anti–CENP-A antibody. The size in the parental clone (clone 02b) was 30.7 kb. Mean size and SD in 17 subclones was 31.4 ± 2.4 kb and is indicated by a thick horizontal bar and two thin horizontal bars, respectively. (D) The distribution of centromere position at chromosome Z in 17 independent subclones. The centromere position was defined as the center of peak mass obtained by CENP-A ChIP-seq analysis. Centromere position drifted within 4.2-kb region.

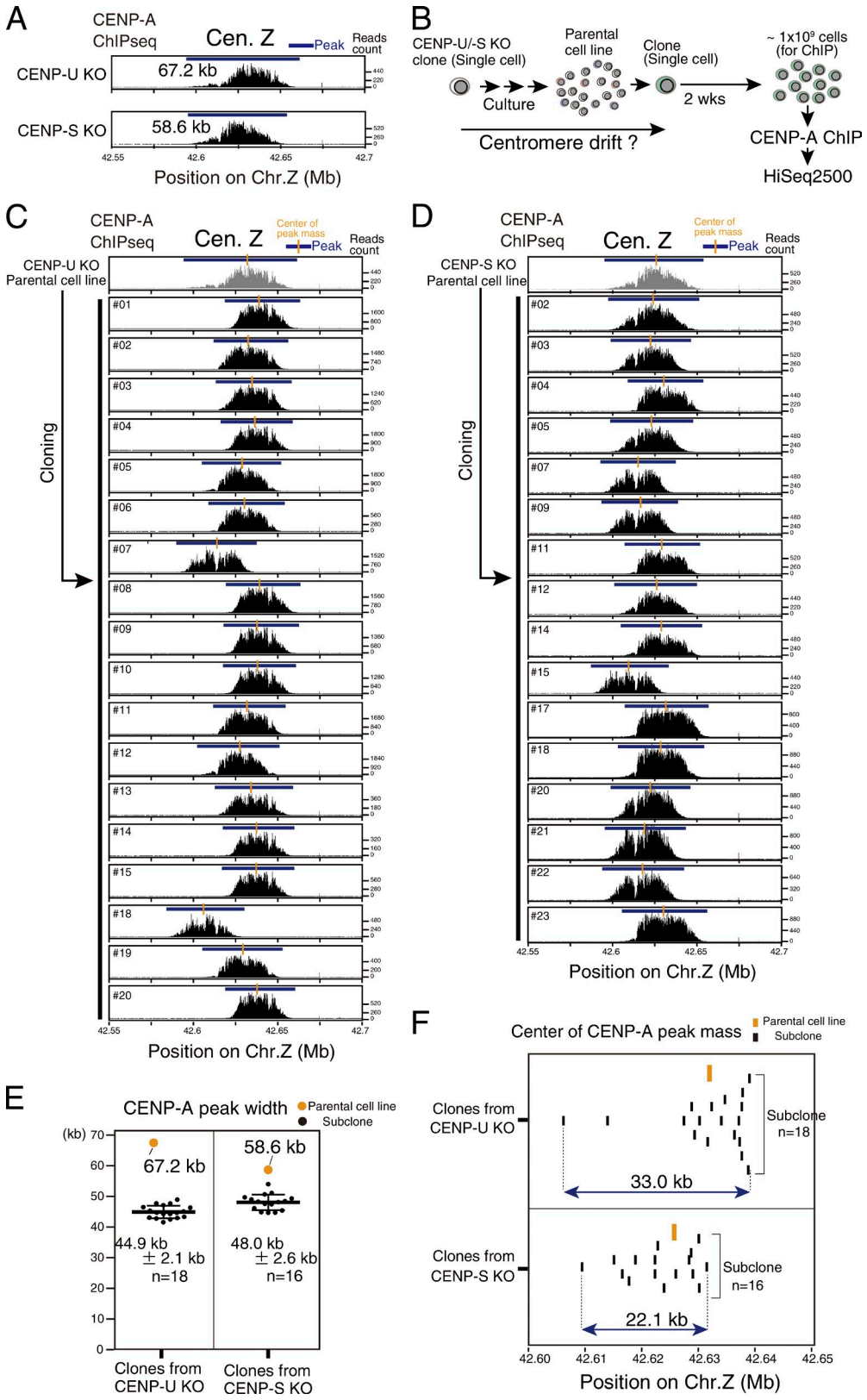

Figure 3. **Centromere drift more frequently occurs in CENP-U– and CENP-S–deficient cells than in the wild-type DT40 cells.** (A) CENP-A ChIP-seq profiles at chicken chromosome Z in CENP-U– and CENP-S–deficient cells. Centromere sizes in CENP-U– and CENP-S–deficient cells were 67.2 and 58.6 kb, respectively. Defined CENP-A peak ranges are indicated by blue bars. (B) Cloning strategy for CENP-U– and CENP-S–deficient cells. The established cell line was cultured, and independent clones were isolated and analyzed using ChIP-seq with anti–CENP-A antibody. (C) CENP-A ChIP-seq profiles in 18 independent CENP-U–deficient clones. The profile of a parental CENP-U–deficient cell line (top) is shown. The independent CENP-U–deficient clones were isolated from these parental CENP-U–deficient cells. Defined CENP-A peak ranges and centers of peak mass are indicated by blue horizontal bars and orange vertical bars, respectively. (D) ChIP-seq profiles of CENP-A on chicken chromosome Z in 16 independent CENP-S–deficient clones. The profile of

where, once the centromere drifts, in the first 16 d, in the presence of tetracycline, the centromere positions are fixed in the subsequent culture in the absence of tetracycline.

We performed similar analyses using CENP-S conditional knockout cells (Fig. S3) and observed that the centromere size increases after the depletion of CENP-S (Fig. S3, B and C), similar to the results obtained using CENP-U conditional knockout cells. Therefore, we demonstrated that 16 d of culturing are sufficient for the detection of centromere drift in CENP-U– or CENP-S–deficient cells.

Centromere CENP-A levels were not increased in CENP-U– or CENP-S–deficient cells

CENP-A–associated region of freshly isolated subclones of wild-type cells should represent a bona fide centromere size. However, because of the technically challenging single-cell ChIP-seq analysis, we are not able to determine whether the observed increase in the centromere size in the subclones of CENP-U– or CENP-S–deficient cells is because of the frequent centromere drift or the centromere–chromatin-wide incorporation of CENP-A in these cells. Nevertheless, we examined CENP-A levels at the kinetochores of CENP-U– or CENP-S–deficient cells.

We have previously shown that the overexpression of HJURP leads to the increase in CENP-A–associated region size (Perpelescu et al., 2015). In this study, we determined that the CENP-A–associated region was increased in CENP-U– or CENP-S–deficient cells. Therefore, we compared the centromeres in HJURP-overexpressing cells with the centromeres in CENP-U–deficient cells. In the HJURP-overexpressing cells, the mean centromere size was determined to be 61.8 kb (Fig. 6 A), greater than the size observed in the wild-type cells, which agrees with the previous observations (Perpelescu et al., 2015). Additionally, this size is similar to the centromere size observed in CENP-U– (67.2 kb) or CENP-S–deficient cells (58.6 kb; Fig. 3).

As HJURP is a CENP-A chaperone, it is possible that the increase in HJURP levels stabilizes CENP-A, which subsequently leads to the increase in total CENP-A amount. As expected, CENP-A amount was significantly higher (1.5 times) in HJURP-overexpressing cells than in the wild-type cells. In contrast to this, the total level of CENP-A did not increase in CENP-U– and CENP-S–deficient cells (Fig. 6 B).

Next, we examined the intensity of CENP-A staining at kinetochore in CENP-U– and CENP-S–deficient and HJU RP-overexpressing cells. CENP-A signal intensities at kinetochores were twofold higher in HJURP-overexpressing cells than in wild-type DT40 cells (Fig. 6, C and D). The levels of other kinetochore proteins were previously shown to increase as well in HJURP-overexpressing cells (Perpelescu et al., 2015). In contrast to this, CENP-A signal intensities at kinetochores in CENP-U– and CENP-S–deficient cells were similar to those in the wild-type cells (Fig. 6, C and D). Therefore, we conclude that centromeric chromatin properties in CENP-U–deficient cells differ from the chromatin properties in HJURP-overexpressing cells, although the increase in CENP-A–associated region of CENP-U– or CENP-S–deficient cells was similar to that in HJURP-overexpressing cells. CENP-A expression levels did not increase in CENP-U– and CENP-S–deficient cells, and the centromere size in these cells may be similar to that in wild-type cells. Therefore, this indicates that the centromere drift frequently occurs in CENP-U– and CENP-S–deficient cells.

CENP-U or CENP-S deficiency leads to the formation of unstable CCAN structure

Because the observed centromere drift in CENP-U– and CENP-S–deficient cells occurs more frequently than in the wild-type cells, CCAN organization in these cells may be different. We performed immunofluorescence analysis using anti–CENP-H, anti–CENP-U, and anti–CENP-S antibodies and wild-type DT40, CENP-U–deficient, CENP-S–deficient, and HJURP-overexpressing cells (Fig. 7 A). The levels of all investigated CCAN proteins were shown to be increased in HJU RP-overexpressing cells (Fig. 7 B), which is consistent with previously obtained results (Perpelescu et al., 2015), suggesting that centromere expansion is caused by the increase in the levels of CCAN components in these cells. CENP-H and CENP-U levels were reduced in CENP-S–deficient cells (Fig. 7 B), suggesting that a complete CCAN structure is not formed in these cells.

Although both CENP-U– and CENP-S–deficient cells are viable, CCAN protein composition was shown to be somewhat different. CENP-H level in CENP-U–deficient cells was similar to that in the wild-type cells. However, the stability of CCAN proteins was examined in a salt-extraction experiment (Fig. 7 C), and we demonstrated that CENP-H, CENP-I, and CENP-K (but not CENP-T, CENP-C, and CENP-A) can be extracted at a lower salt concentration in CENP-U–deficient cells than in the wild-type cells (Fig. 7 D and Fig. S5 B), suggesting that CENP-H–associated proteins are less stable in CENP-U–deficient cells than in the wild-type cells.

Although CENP-I, CENP-L, and CENP-N are major CCAN components, the complete knockout of these proteins is lethal (Okada et al., 2006), and it is difficult to examine centromere drift in these knockout cells. However, single allele depletion may reduce the expression level of CCAN components, which may lead to an unstable CCAN organization. During the generation of complete knockout cells, we maintained freshly frozen stocks of CENP-I (−/−/+; DT40 cells have three copies of CENP-I), CENP-L (−/+), and CENP-N (−/+) cells. These cells were analyzed by ChIP-seq with anti–CENP-A antibody (Fig. S4, A–C). However, CENP-A–associated regions in these cells did not increase, together with the levels of CENP-H and CENP-U, which remained the same as in the wild-type cells (Fig. S4 B), indicating that CCAN organization is almost normal in the investigated CENP-I (−/−/+), CENP-L (−/+), and CENP-N (−/+) cells.

a parental CENP-S–deficient cell line (top) is shown. The independent CENP-S–deficient clones were isolated from the parental CENP-S–deficient cells. Defined CENP-A peak ranges and centers of peak mass are indicated by blue horizontal bars and orange vertical bars, respectively. (E) Centromere size in the subclones of CENP-U– and CENP-S–deficient cells. Centromere size in the parental CENP-U– and CENP-S–deficient cells was 67.2 and 58.6 kb, respectively. Mean centromere sizes and SDs in the subclones of CENP-U– and CENP-S–deficient cell lines were 44.9 ± 2.1 kb (n = 18) and 48.0 ± 2.6 kb (n = 16), respectively. Means and SDs are indicated by a thick horizontal bar and two thin horizontal bars, respectively. (F) The distribution of centromere position on chromosome Z in the 18 and 16 independent subclones of CENP-U– and CENP-S–deficient cells, respectively. Centromere position was defined as a center of peak mass obtained by CENP-A ChIP-seq analysis. Centromere position in CENP-U– and CENP-S–deficient subclones drifted in 33.0- and 22.1-kb regions, respectively. KO, knockout.

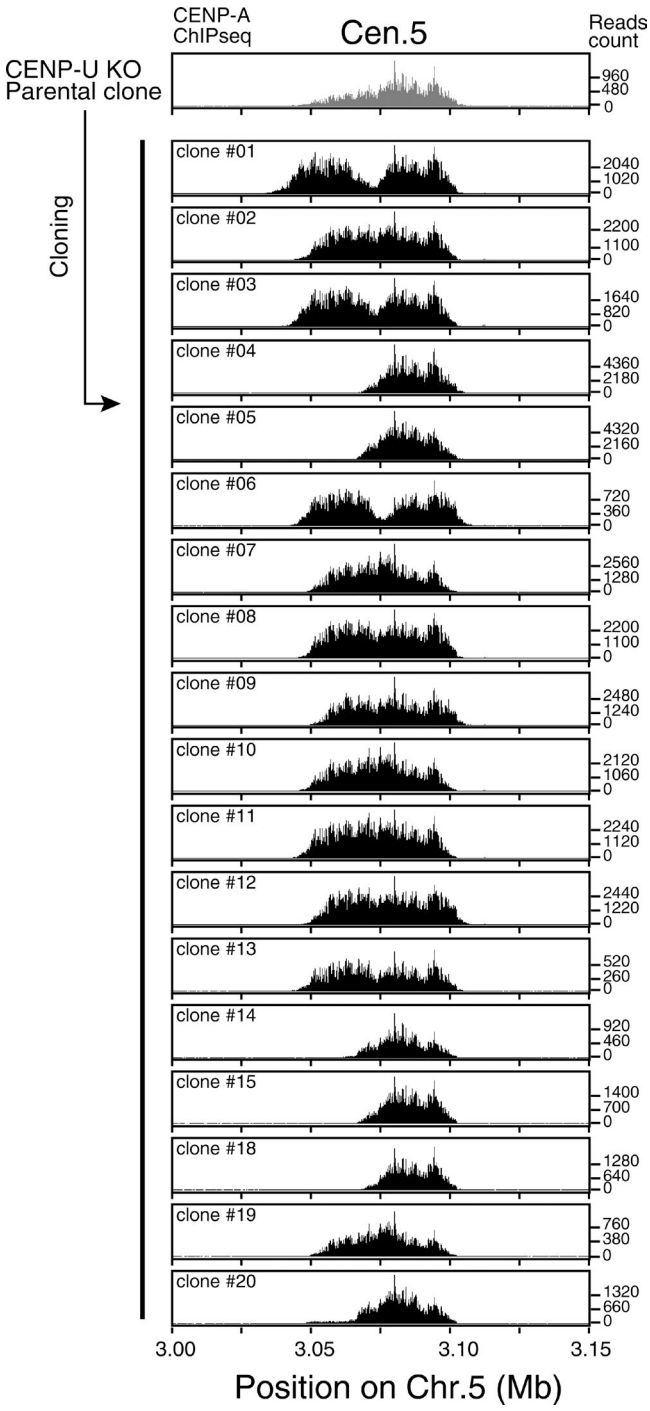

Figure 4. **Centromere drift is observed on chromosome 5 in CENP-U–deficient cells.** CENP-A ChIP-seq profiles on chromosome 5 in 18 independent CENP-U–deficient clones. The profile on chromosome 5 of a parental CENP-U–deficient cell line (top) is shown. Clear double peaks are observed in clones 01, 03, 06, 08, and 13. KO, knockout.

We previously isolated clones in which a neocentromere was formed on chromosome 5 after deletion of a native centromere 5 in DT40 cells (Shang et al., 2013). As DT40 has two copies of chromosome 5, we can compare size of CENP-A–associated regions in neocentromere and native centromere for chromosome 5 (Fig. S4 D). Interestingly, centromere sizes of neocentromeres are always longer than those of native centromeres (Fig. S4 D). As neocentromeres are newly created, CCAN proteins may not be properly fixed in neocentromeres, which may cause frequent centromere drift in fresh neocentromeres.

The obtained data showed that CENP-H complex proteins are not normally associated with centromeres in CENP-U– and CENP-S–deficient cells (Fig. 7 and Fig. S5, A and B), and this suggests that the incomplete formation of CCAN causes a frequent centromere drift. However, CENP-U or CENP-S may be localized at the boundaries between centromere and noncentromere regions to prevent centromere drift. To test this possibility, we performed CENP-U or CENP-S ChIP-seq analysis (Fig. S5 C). CENP-U or CENP-S ChIP-seq profiles were shown to be similar to the CENP-A profile, suggesting that CENP-U or CENP-S is not enriched at the boundaries between the centromere and noncentromere regions (Fig. S5 C).

The obtained data suggest that CCAN is partially disturbed in CENP-U– and CENP-S–deficient cells, and this incomplete structure may cause a frequent centromere drift in these cells.

Discussion

Chicken DT40 cells contain a nonrepetitive centromere at a single copy of chromosome Z, and these cells can be relatively easily manipulated. Therefore, they represent one of the best systems for the systematic analysis of centromere drift at base-pair resolution. In this study, we used these cells and demonstrated that centromere drift occurs over a large number of cell divisions, but the centromere position is relatively stable within at least 2 wk of culture (∼50 cell divisions).

The determination of centromere size and position is difficult without single-cell analyses, but the application of ChIP-seq technique for single-cell analyses is currently limited. Therefore, we isolated multiple single clones and immediately characterized them. To perform these analyses, it is necessary to culture these cells for at least 2 wk from a single cell (Figs. 1 C, 2 A, and 3 B). We confirmed that the size and position of CENP-A–associated regions did not change in the wild-type cells during 2 wk of culturing, and therefore, we believe that our cloning and ChIP-seq strategy is feasible, reliable, and appropriate for the observation of the centromere drift. Although we cannot completely rule out the possibility that centromere size and position vary in each single cell, they are relatively constant among subclones isolated from a single DT40 cell (clone 02b) in 2-wk culture (Fig. 2). Based on the analyses of 17 independent subclones, we estimated the size of chromosome Z centromere to be ∼31 kb, which is equivalent to the centromere size measured in the parental clone 02b cell (30.7 kb).

Generally, centromere drift is deleterious for cells, because the formation of centromeres may potentially inactivate the expression of crucial genes. However, as centromere position is defined by sequence-independent epigenetic mechanisms, this drift may represent a naturally occurring event. The repetitive DNA array may provide a safety buffer for the centromere drift (Fukagawa and Earnshaw, 2014a). In addition to these repetitive arrays, different mechanisms for the suppression of centromere drift may exist in the cell. Our data indicate that the centromere position can drift after a large number of cell divisions, but the drift is normally suppressed.

The obtained results suggest that the complete CCAN structure contributes to the suppression of centromere drift (Fig. S5, D–F). Currently, although the detailed molecular mechanism of this process remains unclear, the precise CENP-A incorporation into a correct position at the chromosome must be crucial for the

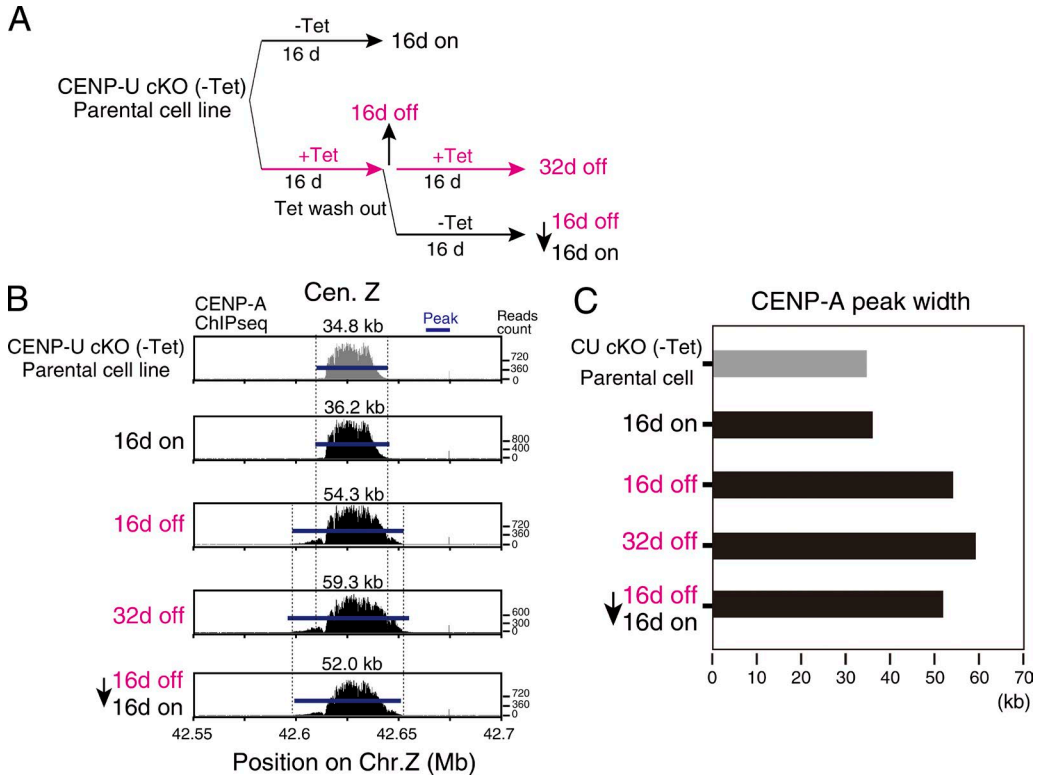

Figure 5. **CENP-U deficiency–dependent increase in CENP-A–associated region size.** (A) ChIP-seq samples were prepared using CENP-U conditional knockout (cKO) cells. In the presence of tetracycline (Tet), CENP-U expression is suppressed. CENP-U conditional knockout cells were cultured in the absence (–Tet) or presence (+Tet) of tetracycline. "16d on" indicates a 16-d culture in the absence of tetracycline, whereas "16d off" indicates a 16-d culture in the presence of tetracycline. (B) CENP-A–associated region size measured in the samples indicated in A, based on ChIP-seq analysis with anti–CENP-A antibody. CENP-A–associated region sizes of the parental CENP-U conditional knockout (CU cKO) cells, 16 d on cells, 16 d off cells, 32 d off cells, and 16 d off/16 d on cells were 34.8, 36.2, 54.3, 59.3, and 52.0 kb, respectively. Defined CENP-A–associated region sizes are indicated by blue bars. (C) Graphical representation of the centromere size in samples shown in B.

suppression of centromere drift. We have previously shown that CCAN members CENP-H or CENP-I are essential for the deposition of newly synthesized CENP-A (Okada et al., 2006, 2009). It is possible that CCAN may function as a marker for new CENP-A deposition and that CENP-A must be incorporated into the existing centromere position. As CENP-H– and CENP-I–deficient cells are not viable, we could not test the centromere drift in these deficient cells. However, as CENP-U and CENP-S are associated with the CENP-H complex, including CENP-H, -I, and -K, it is possible that CENP-A incorporation into the correct chromosomal position may not occur because of the altered activity of CENP-H complex in CENP-U– and CENP-S–deficient cells (Fig. S5 E). Alternatively, because CCAN structure is not complete, it is possible that this network is unstable and not tightly associated with centromere chromatin, which may cause the centromere drift. CCAN is known to function as a platform to recruit outer kinetochore proteins for ensuring microtubule attachment (McKinley and Cheeseman, 2016). In this study, we determined an additional role of CCAN in the establishment of normal centromere chromatin, which contributes to the suppression of centromere drift.

Materials and methods

Cell culture

DT40 cells were cultured in DMEM (Sigma-Aldrich) supplemented with 10% FBS (Hana-Nesco Bio Corp.), 1% chicken serum (Gibco), 100 units/ml penicillin/100 µg/ml streptomycin (Gibco), and 20 µM 2-mercaptoethanol (Sigma-Aldrich) in 5% CO_2 at 38.5°C under saturated humidity (Hori et al., 2008a). Plasmids for drug-resistance genes (pBS134 for blasticidin and pBS250 for histidinol) were transfected into cells with a Gene Pulser II electroporator (Bio-Rad Laboratories) into DT40 cells to perform the cloning, and single colonies were isolated. CENP-U knockout cells were generated by replacement of exons 4–7 with drug-resistant genes (Minoshima et al., 2005). The CENP-U cDNA construct under control of a tetracycline promoter was randomly integrated into CENP-U knockout cells to generate CENP-U conditional knockout cells. CENP-S knockout cells were generated by replacement of entire exons with drug-resistant genes (Amano et al., 2009). The CENP-S cDNA construct under control of the tetracycline promoter was randomly integrated into CENP-S knockout cells to generate CENP-S conditional knockout cells.

ChIP-seq analysis

Nuclei were isolated from 1.5 × 10^9 DT40 cells and digested with 60 units/ml MNase (Takara Bio Inc.) in buffer A (15 mM Hepes-KOH, pH 7.4, 15 mM NaCl, 60 mM KCl, 1 mM $CaCl_2$, 0.34 M sucrose, 0.5 mM spermidine, 0.15 mM spermine, 1 mM DTT, and 1× complete protease inhibitor cocktail; Roche). After centrifugation at 17,800 *g* for 5 min, the chromatin pellet was suspended with buffer B (20 mM Tris-HCl, pH 8.0, 0.5 M NaCl, 10 mM EDTA, and 1× complete protease inhibitor cocktail; Roche), and then mononucleosome was extracted. The extracted mononucleosome fraction was incubated for 2 h at 4°C with Protein G Sepharose beads (GE Healthcare), which were preincubated

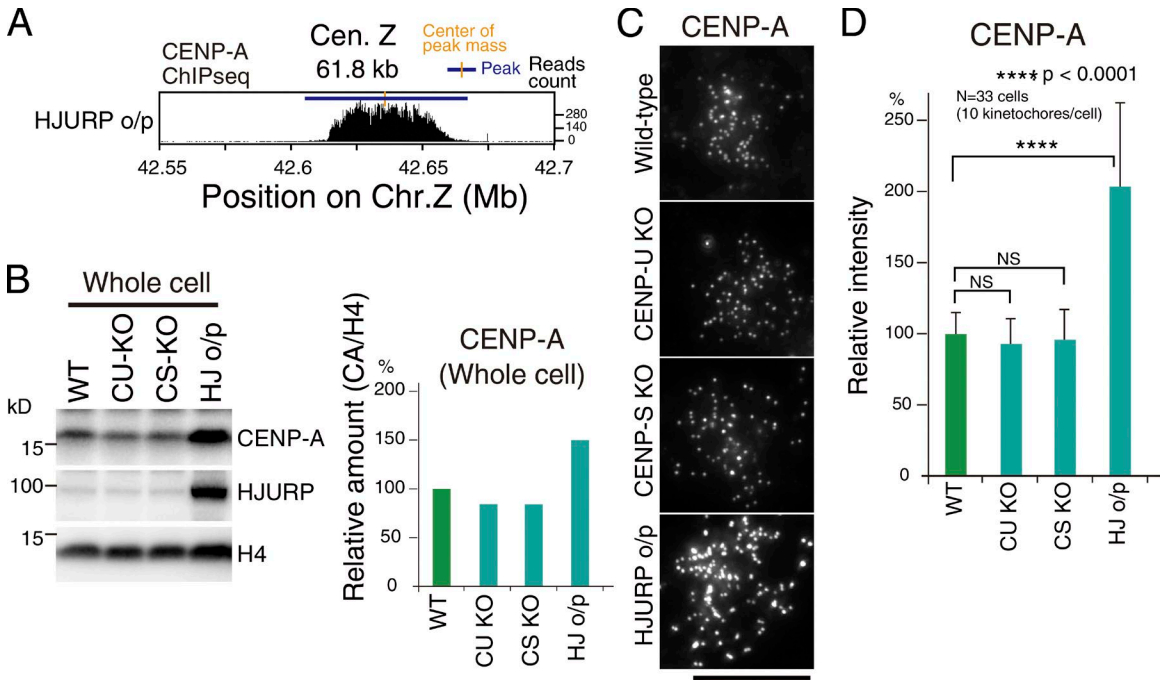

Figure 6. **Size of centromere region increases in CENP-U– or CENP-S–deficient cells, whereas the amount of CENP-A remains the same as in the wild-type cells.** (A) ChIP-seq profile of CENP-A on chicken chromosome Z in HJURP-overexpressing cell. Centromere size in HJURP-overexpressing cell was 61.8 kb. Defined CENP-A peak range and center of peak mass are indicated by a blue horizontal bar and an orange vertical bar, respectively. (B) Western blot analysis of the whole-cell extracts of wild-type (WT) DT40, CENP-U–deficient (CU-knockout [-KO]), CENP-S–deficient (CS-KO), and HJURP-overexpressing (HJ o/p) cells, using anti–CENP-A, anti-HJURP, and anti–histone H4 antibodies. Independent experiments were performed three times. Band intensities of CENP-A measured and normalized to histone H4 intensities in each extract are shown. (C) Immunofluorescence analysis of wild-type DT40, CENP-U–deficient, CENP-S–deficient, and HJURP-overexpressing cells using anti–CENP-A antibody. Bar, 10 µm. (D) The analysis of CENP-A signal intensity at kinetochores in wild-type DT40, CENP-U–deficient, CENP-S–deficient, and HJURP-overexpressing cells. Experiments were performed in C. Signal intensities of 10 kinetochores in each cell were measured (n = 33). Error bars indicate SD. Statistical analyses were performed by a one-sided Student's t test. ****, P < 0.0001 is defined as significant.

with rabbit polyclonal anti–chicken CENP-A antibody (Régnier et al., 2003). Beads were washed with buffer B four times, and the bound DNA was purified by phenol-chloroform extraction and ethanol precipitation. The purified DNA was analyzed on a DNA sequencer (HiSeq 2500; Illumina). ChIP-seq libraries were constructed with the TruSeq DNA LT Sample Prep kit (Illumina) as described in the protocols provided with the kit. In brief, ∼50 ng of purified DNA was end-repaired, followed by the addition of a single adenosine nucleotide at 3′ and ligation to the universal library adapters. DNA was amplified by eight PCR cycles, and the DNA libraries were prepared. ChIP DNA libraries were sequenced using the HiSeq 2500 in up to 2 × 151 cycles. Image analysis and base calling were performed with the standard pipeline version RTA1.17.21.3 (Illumina).

Sequencing data were mapped to chicken genome database galGal4 (UCSC Genome Browser) with a BWA 0.6.2 mapping tool (Li and Durbin, 2009).

Immunofluorescence

For immunofluorescence analysis of centromere proteins, DT40 cells were treated with hypotonic buffer (20 mM Tris-HCl, pH 7.4, and 1.5 mM KCl) at room temperature for 10 min and cytospin-deposited into glass slides. The samples were fixed in cold methanol for 20 min at −20°C for detection of CENP-A, CENP-S, and CENP-U or fixed in 3% PFA for 10 min and permeabilized in 0.5% NP-40 in PBS for 10 min for detection of CENP-H. Afterward, the samples were treated with 0.5% BSA in PBS for 5 min and different primary rabbit polyclonal antibodies: anti–chicken CENP-A (Régnier et al., 2003), CENP-H (Fukagawa et al., 2001), CENP-S (Amano et al., 2009), and CENP-U (Minoshima et al., 2005) were incubated for 1 h at 1:1,000 dilution in 0.5% BSA in PBS. After washing three times with 0.5% BSA in PBS, FITC-conjugated goat anti–rabbit IgG ($F[ab']_2$; Jackson ImmunoResearch Laboratories, Inc.) was incubated for 30 min at 1:1,000 dilution in 0.5% BSA in PBS. Samples were counterstained with 1 µg/ml DAPI and mounted with mounting medium (VECTASIELD; Vector Laboratories). Immunofluorescence images were obtained using a spinning disk confocal microscope system (CV1000; Yokogawa Electric Corporation) and ×100/1.4 NA oil iris objective lens (Olympus). Data analyses were performed with Metamorph software (Molecular Devices). Signal intensities were calculated by a method developed by Hoffman et al. (2001).

FISH analysis

After treatment of 100 ng/ml nocodazole (Sigma-Aldrich) for 2 h to increase mitotic index, DT40 cells were treated with hypotonic buffer (20 mM Hepes-KOH, pH 7.4, 40 mM KCl, and 0.5 mM EDTA) for 10 min at 37°C and fixed in ice-cold methanol/acetic acid (3:1) solution. Fixed DT40 cells were dropped onto glass slides to prepare mitotic chromosome spreads. Chromosomes were dehydrated in ethanol, and chromosome DNAs were denatured in denaturing buffer (2× SSC and 70% formamide) for 2 min at 70°C. The pFN-1 plasmid DNA possessing a 24-kb Z-specific macrosatellite repeat unit (Hori et al., 1996) was labeled with Biotin-16-dUTP (Roche) by nick translation to yield a FISH probe. Partial sequence information of the 24-kb DNA was deposited in the DNA Data Bank of Japan database under accession no. D63169. The DNA probe was dissolved in a hybridization buffer (40 mM phosphate buffer, pH 7.0, 2 × SSC,

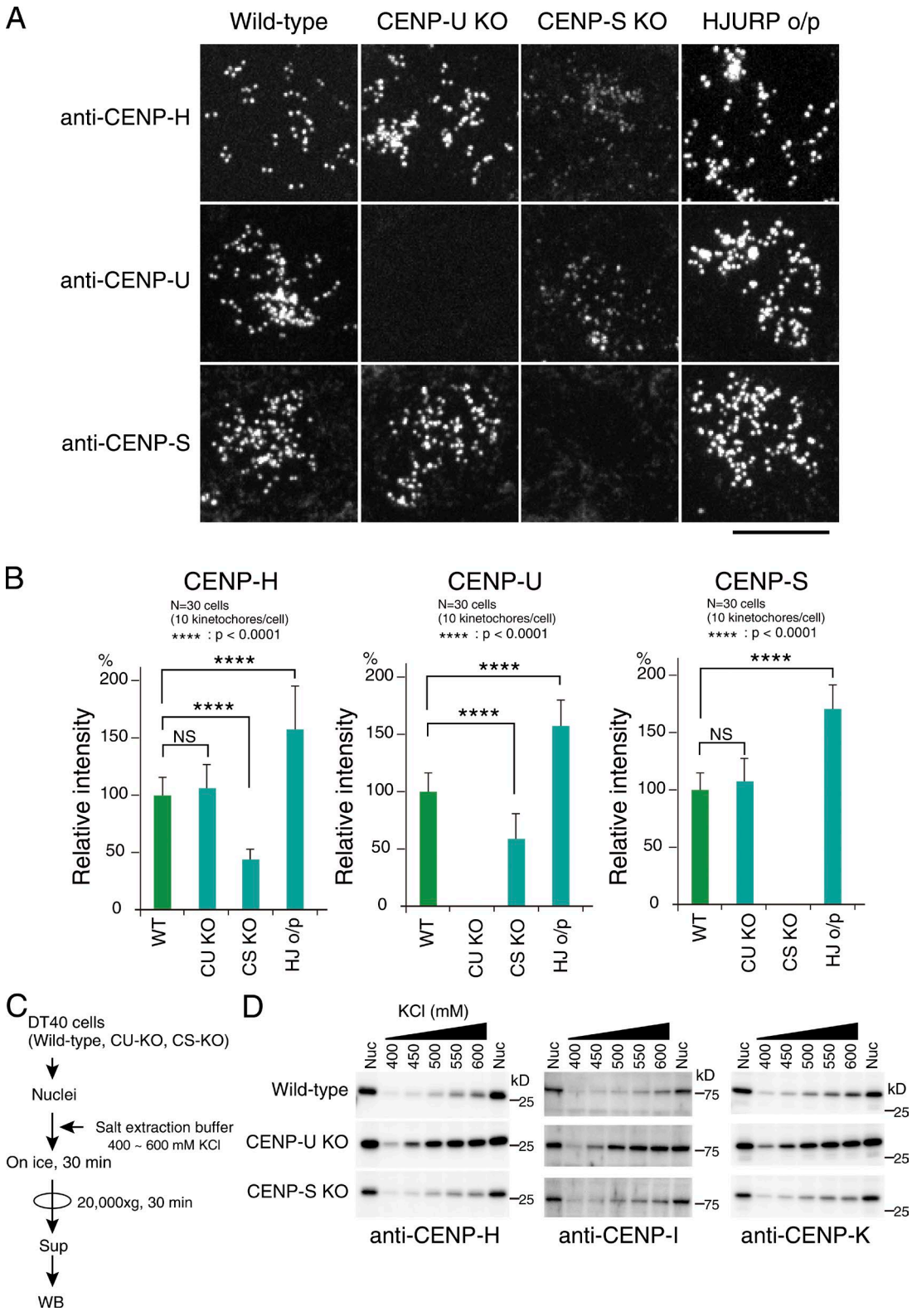

Figure 7. **CENP-U or CENP-S deficiency affects CCAN stability.** (A) Immunofluorescence analysis of wild-type DT40, CENP-U–deficient, CENP-S–deficient, and HJURP-overexpressing cells, using anti–CENP-H, anti–CENP-U, and anti–CENP-S antibodies. Bar, 10 µm. (B) Analysis of CENP-H, CENP-U, and CENP-S signal intensities at wild-type (WT) DT40, CENP-U–deficient (CU KO), CENP-S–deficient (CS KO), and HJURP-overexpressing (HJ o/p) cell kinetochores, based on the immunofluorescence analysis performed in A. Signal intensities of 10 kinetochores in each cell were measured (n = 30). Error bars indicate SD. Statistical analyses were performed by a one-sided Student's t test. ****, $P < 0.0001$ is defined as significant. (C) Experimental design of CCAN protein salt extraction. Sup, Supernatant; WB, Western blot analysis. (D) Western blot analysis of the cell extracts using the indicated salt concentrations and anti–CENP-H, anti–CENP-I, and anti–CENP-K antibodies. Independent salt extraction experiments were performed three times. Nuc, isolated whole nuclei before salt extraction.

50% formamide, 10% dextran sulfate, 1× Denhart's solution, 100 µg/ml salmon sperm DNA, and 0.5 mM EDTA) and denatured for 10 min at 75°C. Hybridization was performed in a humidity chamber overnight at 37°C. Slides were washed once in 2× SSC, twice in 50% formamide in 2× SSC, and twice in 0.1× SSC for 5 min each at 42°C. After washing out probes, slides were incubated with Cy3-conjugated streptavidin (GE Healthcare) at 1:1,000 dilution in 1% BSA and 0.05% Tween 20 in 4× SSC for 30 min at 37°C. Samples were counterstained with 1 µg/ml DAPI and mounted with VECTASIELD mounting medium. Fluorescence images were obtained using a Cool SNAP HQ 2 camera (Roper Technologies) mounted on an IX71 inverted microscope with UPlanApo ×100/1.35 NA oil iris objective lens (Olympus) and a filter wheel. Image acquisition and data analyses were performed using Metamorph software.

Salt-extraction experiment

Wild-type or CENP-U– or -S–deficient DT40 cells (5×10^7 cells) were suspended in 1 ml ice-cold TMS (10 mM Tris-HCl, pH 7.5, 5 mM $MgCl_2$, and 0.25 M sucrose), centrifuged (640 *g*, 10 min, 4°C), and resuspended in 1 ml ice-cold TMS-Triton (TMS, 0.5% Triton X-100, and complete protease inhibitor cocktail; Roche). After a 5-min incubation on ice, nuclei were collected by centrifugation (2,000 *g*, 10 min, 4°C), washed with 1 ml TMS-Triton (2,000 *g*, 10 min, 4°C), and resuspended in 0.5 ml TMS-Triton. 50 µl nuclear suspension was added to 450 µl salt-extraction buffer (20 mM Hepes-KOH, pH 7.4, 25% glycerol, 1.5 mM $MgCl_2$, 0.2 mM EDTA, pH 8.0, 0.5 mM DTT, and complete protease inhibitor cocktail; Roche) containing 200–800 mM KCl as a final concentration and incubated on ice for 30 min. After centrifugation (20,000 *g*, 30 min, 4°C), the supernatant was collected and used for Western blotting analysis.

Western blot analysis

DT40 cells were harvested and lysed with SDS sample buffer (50 mM Tris-HCl, pH 6.8, 2% SDS, 10% glycerol, 5% [wt/vol] 2-mercaptoethanol, and 0.005% [wt/vol] bromophenol blue [MP Biomedicals]). Cell lysates or nuclear protein samples obtained through salt-extraction experiments were separated by 10–20% gradient SDS-PAGE and transferred to FluoroTrans PVDF membrane (Pall Corporation). After blocking with 5% nonfat milk in TBST (10 mM Tris-HCl, pH 7.5, 150 mM NaCl, and 0.1% [wt/vol] Tween 20), membranes were incubated with primary antibodies at 1:5,000 dilutions in Solution 1 (Can Get Signal; Toyobo). After washing three times with TBST, membranes were incubated with HRP-conjugated anti–rabbit IgG or –mouse IgG antibodies (Jackson ImmunoResearch Laboratories, Inc.) at 1:15,000 dilution in Solution 2 (Can Get Signal). The signals were developed by ECL Prime Western Blotting Detection Reagent (GE Healthcare), and blot images were obtained using Chemi-Doc Touch imaging system (Bio-Rad Laboratories). Data analyses were performed with Image Lab (Bio-Rad Laboratories). Primary antibodies anti–chicken CENP-A (Régnier et al., 2003), CENP-H (Fukagawa et al., 2001), CENP-I (Nishihashi et al., 2002), CENP-K (Okada et al., 2006), and HJURP (Perpelescu et al., 2015) rabbit antibodies and mouse anti–histone H4 mAb (200a9c5; Hayashi-Takanaka et al., 2015) were used.

Statistical analysis

Peak width values for CENP-A–associated regions were shown as mean ± SD. Significances of statistical differences between two groups of immunofluorescence intensities were evaluated by a one-sided Student's *t* test. A p-value <0.0001 is defined as significant. Data distribution was assumed to be normal, but this was not formally tested.

Online supplemental material

Fig. S1 shows the definition of centromere region based on ChIP-seq. Fig. S2 shows the characterization of clones, which were used for centromere drift analysis. Fig. S3 provides an analysis of centromere region in CENP-S conditional knockout cells. Fig. S4 is an analysis of centromere region in CENP-I (−/−/+), CENP-L (−/+), and CENP-N (−/+) cells and cells with neocentromere on chromosome 5. Fig. S5 shows salt-extraction experiments of CCAN proteins, ChIP-seq with CENP-U and CENP-S, and a summary of this study.

Acknowledgments

The authors thank S. Teramoto, Y. Fukagawa, and R. Fukuoka for technical assistance.

This work was supported by the Japan Society for the Promotion of Science Grants-in-Aid for Scientific Research (KAKENHI) JP25221106, JP16H06279, and JP15H05972 to T. Fukagawa and JP26440190, JP25116002, and JP15H01477 to T. Hori.

The authors declare no competing financial interests.

Author contributions: T. Hori performed the entire experiments and analyzed the data. N. Kagawa helped with various ChIP experiments. A. Toyoda and A. Fujiyama performed deep sequencing. S. Misu, N. Monma, and K. Ikeo analyzed deep sequencing data. F. Makino contributed to data analyses. T. Hori and T. Fukagawa designed all experiments and wrote the paper.

Submitted: 1 May 2016
Revised: 12 September 2016
Accepted: 11 November 2016

References

Allshire, R.C., and G.H. Karpen. 2008. Epigenetic regulation of centromeric chromatin: Old dogs, new tricks? *Nat. Rev. Genet.* 9:923–937. http://dx.doi.org/10.1038/nrg2466

Amano, M., A. Suzuki, T. Hori, C. Backer, K. Okawa, I.M. Cheeseman, and T. Fukagawa. 2009. The CENP-S complex is essential for the stable assembly of outer kinetochore structure. *J. Cell Biol.* 186:173–182. http://dx.doi.org/10.1083/jcb.200903100

Black, B.E., and D.W. Cleveland. 2011. Epigenetic centromere propagation and the nature of CENP-a nucleosomes. *Cell.* 144:471–479. http://dx.doi.org/10.1016/j.cell.2011.02.002

Dunleavy, E.M., D. Roche, H. Tagami, N. Lacoste, D. Ray-Gallet, Y. Nakamura, Y. Daigo, Y. Nakatani, and G. Almouzni-Pettinotti. 2009. HJURP is a cell-cycle-dependent maintenance and deposition factor of CENP-A at centromeres. *Cell.* 137:485–497. http://dx.doi.org/10.1016/j.cell.2009.02.040

du Sart, D., M.R. Cancilla, E. Earle, J.I. Mao, R. Saffery, K.M. Tainton, P. Kalitsis, J. Martyn, A.E. Barry, and K.H. Choo. 1997. A functional neo-centromere formed through activation of a latent human centromere and consisting of non-alpha-satellite DNA. *Nat. Genet.* 16:144–153. http://dx.doi.org/10.1038/ng0697-144

Foltz, D.R., L.E. Jansen, A.O. Bailey, J.R. Yates III, E.A. Bassett, S. Wood, B.E. Black, and D.W. Cleveland. 2009. Centromere-specific assembly of CENP-a nucleosomes is mediated by HJURP. *Cell.* 137:472–484. http://dx.doi.org/10.1016/j.cell.2009.02.039

Fukagawa, T., and W.C. Earnshaw. 2014a. The centromere: Chromatin foundation for the kinetochore machinery. *Dev. Cell.* 30:496–508. http://dx.doi.org/10.1016/j.devcel.2014.08.016

Fukagawa, T., and W.C. Earnshaw. 2014b. Neocentromeres. *Curr. Biol.* 24:R946–R947. http://dx.doi.org/10.1016/j.cub.2014.08.032

Fukagawa, T., Y. Mikami, A. Nishihashi, V. Regnier, T. Haraguchi, Y. Hiraoka, N. Sugata, K. Todokoro, W. Brown, and T. Ikemura. 2001. CENP-H, a constitutive centromere component, is required for centromere targeting

of CENP-C in vertebrate cells. *EMBO J.* 20:4603–4617. http://dx.doi.org/10.1093/emboj/20.16.4603

Gent, J.I., K. Wang, J. Jiang, and R.K. Dawe. 2015. Stable patterns of CENH3 occupancy through maize lineages containing genetically similar centromeres. *Genetics.* 200:1105–1116. http://dx.doi.org/10.1534/genetics.115.177360

Hayashi-Takanaka, Y., K. Maehara, A. Harada, T. Umehara, S. Yokoyama, C. Obuse, Y. Ohkawa, N. Nozaki, and H. Kimura. 2015. Distribution of histone H4 modifications as revealed by a panel of specific monoclonal antibodies. *Chromosome Res.* 23:753–766. http://dx.doi.org/10.1007/s10577-015-9486-4

Hoffman, D.B., C.G. Pearson, T.J. Yen, B.J. Howell, and E.D. Salmon. 2001. Microtubule-dependent changes in assembly of microtubule motor proteins and mitotic spindle checkpoint proteins at PtK1 kinetochores. *Mol. Biol. Cell.* 12:1995–2009. http://dx.doi.org/10.1091/mbc.12.7.1995

Hori, T., Y. Suzuki, I. Solovei, Y. Saitoh, N. Hutchison, J.E. Ikeda, H. Macgregor, and S. Mizuno. 1996. Characterization of DNA sequences constituting the terminal heterochromatin of the chicken Z chromosome. *Chromosome Res.* 4:411–426. http://dx.doi.org/10.1007/BF02265048

Hori, T., M. Amano, A. Suzuki, C.B. Backer, J.P. Welburn, Y. Dong, B.F. McEwen, W.H. Shang, E. Suzuki, K. Okawa, et al. 2008a. CCAN makes multiple contacts with centromeric DNA to provide distinct pathways to the outer kinetochore. *Cell.* 135:1039–1052. http://dx.doi.org/10.1016/j.cell.2008.10.019

Hori, T., M. Okada, K. Maenaka, and T. Fukagawa. 2008b. CENP-O class proteins form a stable complex and are required for proper kinetochore function. *Mol. Biol. Cell.* 19:843–854. http://dx.doi.org/10.1091/mbc.E07-06-0556

Li, H., and R. Durbin. 2009. Fast and accurate short read alignment with Burrows-Wheeler transform. *Bioinformatics.* 25:1754–1760. http://dx.doi.org/10.1093/bioinformatics/btp324

Lomiento, M., F. Grasser, M. Rocchi, and S. Müller. 2013. The interplay between genome organization and nuclear architecture of primate evolutionary neo-centromeres. *Genomics.* 102:288–295. http://dx.doi.org/10.1016/j.ygeno.2013.04.017

Marshall, O.J., A.C. Chueh, L.H. Wong, and K.H. Choo. 2008. Neocentromeres: New insights into centromere structure, disease development, and karyotype evolution. *Am. J. Hum. Genet.* 82:261–282. http://dx.doi.org/10.1016/j.ajhg.2007.11.009

McKinley, K.L., and I.M. Cheeseman. 2016. The molecular basis for centromere identity and function. *Nat. Rev. Mol. Cell Biol.* 17:16–29. http://dx.doi.org/10.1038/nrm.2015.5

Minoshima, Y., T. Hori, M. Okada, H. Kimura, T. Haraguchi, Y. Hiraoka, Y.C. Bao, T. Kawashima, T. Kitamura, and T. Fukagawa. 2005. The constitutive centromere component CENP-50 is required for recovery from spindle damage. *Mol. Cell. Biol.* 25:10315–10328. http://dx.doi.org/10.1128/MCB.25.23.10315-10328.2005

Nishihashi, A., T. Haraguchi, Y. Hiraoka, T. Ikemura, V. Regnier, H. Dodson, W.C. Earnshaw, and T. Fukagawa. 2002. CENP-I is essential for centromere function in vertebrate cells. *Dev. Cell.* 2:463–476. http://dx.doi.org/10.1016/S1534-5807(02)00144-2

Okada, M., I.M. Cheeseman, T. Hori, K. Okawa, I.X. McLeod, J.R. Yates III, A. Desai, and T. Fukagawa. 2006. The CENP-H-I complex is required for the efficient incorporation of newly synthesized CENP-A into centromeres. *Nat. Cell Biol.* 8:446–457. http://dx.doi.org/10.1038/ncb1396

Okada, M., K. Okawa, T. Isobe, and T. Fukagawa. 2009. CENP-H-containing complex facilitates centromere deposition of CENP-A in cooperation with FACT and CHD1. *Mol. Biol. Cell.* 20:3986–3995. http://dx.doi.org/10.1091/mbc.E09-01-0065

Perpelescu, M., and T. Fukagawa. 2011. The ABCs of CENPs. *Chromosoma.* 120:425–446. http://dx.doi.org/10.1007/s00412-011-0330-0

Perpelescu, M., T. Hori, A. Toyoda, S. Misu, N. Monma, K. Ikeo, C. Obuse, A. Fujiyama, and T. Fukagawa. 2015. HJURP is involved in the expansion of centromeric chromatin. *Mol. Biol. Cell.* 26:2742–2754. http://dx.doi.org/10.1091/mbc.E15-02-0094

Purgato, S., E. Belloni, F.M. Piras, M. Zoli, C. Badiale, F. Cerutti, A. Mazzagatti, G. Perini, G. Della Valle, S.G. Nergadze, et al. 2015. Centromere sliding on a mammalian chromosome. *Chromosoma.* 124:277–287. (published erratum appears in *Chromosoma.* 2015. 124:289) http://dx.doi.org/10.1007/s00412-014-0493-6

Régnier, V., J. Novelli, T. Fukagawa, P. Vagnarelli, and W. Brown. 2003. Characterization of chicken CENP-A and comparative sequence analysis of vertebrate centromere-specific histone H3-like proteins. *Gene.* 316:39–46. http://dx.doi.org/10.1016/S0378-1119(03)00768-6

Shang, W.H., T. Hori, A. Toyoda, J. Kato, K. Popendorf, Y. Sakakibara, A. Fujiyama, and T. Fukagawa. 2010. Chickens possess centromeres with both extended tandem repeats and short non-tandem-repetitive sequences. *Genome Res.* 20:1219–1228. http://dx.doi.org/10.1101/gr.106245.110

Shang, W.H., T. Hori, N.M. Martins, A. Toyoda, S. Misu, N. Monma, I. Hiratani, K. Maeshima, K. Ikeo, A. Fujiyama, et al. 2013. Chromosome engineering allows the efficient isolation of vertebrate neocentromeres. *Dev. Cell.* 24:635–648. http://dx.doi.org/10.1016/j.devcel.2013.02.009

Voullaire, L.E., H.R. Slater, V. Petrovic, and K.H. Choo. 1993. A functional marker centromere with no detectable alpha-satellite, satellite III, or CENP-B protein: Activation of a latent centromere? *Am. J. Hum. Genet.* 52:1153–1163.

Wade, C.M., E. Giulotto, S. Sigurdsson, M. Zoli, S. Gnerre, F. Imsland, T.L. Lear, D.L. Adelson, E. Bailey, R.R. Bellone, et al. Broad Institute Whole Genome Assembly Team. 2009. Genome sequence, comparative analysis, and population genetics of the domestic horse. *Science.* 326:865–867. http://dx.doi.org/10.1126/science.1178158

Westhorpe, F.G., and A.F. Straight. 2013. Functions of the centromere and kinetochore in chromosome segregation. *Curr. Opin. Cell Biol.* 25:334–340. http://dx.doi.org/10.1016/j.ceb.2013.02.001

Yao, J., X. Liu, T. Sakuno, W. Li, Y. Xi, P. Aravamudhan, A. Joglekar, W. Li, Y. Watanabe, and X. He. 2013. Plasticity and epigenetic inheritance of centromere-specific histone H3 (CENP-A)-containing nucleosome positioning in the fission yeast. *J. Biol. Chem.* 288:19184–19196. http://dx.doi.org/10.1074/jbc.M113.471276